A&A 411, L321–L325 (2003)
DOI: 10.1051/0004-6361:20031232

Astronomy & Astrophysics

INTEGRAL results on GRB 030320: A long gamma-ray burst detected at the edge of the field of view⋆

A. von Kienlin[1], V. Beckmann[2,3], S. Covino[8], D. Götz[4,5], G. G. Lichti[1], D. Malesani[9], S. Mereghetti[4], E. Molinari[8], A. Rau[1], C. R. Shrader[6,7], S. J. Sturner[6,7], and F. Zerbi[8]

[1] Max-Planck-Institut für extraterrestrische Physik, Giessenbachstrasse, 85748 Garching, Germany
[2] Institut für Astronomie und Astrophysik, Universität Tübingen, Sand 1, 72076 Tübingen, Germany
[3] INTEGRAL Science Data Centre, Chemin d'Écogia 16, 1290 Versoix, Switzerland
[4] Istituto di Astrofisica Spaziale e Fisica Cosmica – CNR, Sezione di Milano "G. Occhialini", via Bassini 15, 20133 Milano, Italy
[5] Dipartimento di Fisica, Università degli Studi di Milano Bicocca, P.zza della Scienza 3, 20126 Milano, Italy
[6] Code 661, NASA/Goddard Space Flight Center, Greenbelt, MD 20771, USA
[7] Universities Space Research Association, 7501 Forbes Blvd. #206, Seabrook, MD 20706, USA
[8] INAF / Brera Astronomical Observatory, via E. Bianchi 23807, Merate (LC), Italy
[9] International School for Advanced Studies (SISSA-ISAS), via Beirut 2–4, 34014 Trieste, Italy

Received 16 July 2003 / Accepted 8 August 2003

Abstract. GRB 030320 is the 5th gamma-ray burst (GRB) detected by INTEGRAL in the field of view (FoV). It is so far the GRB with the largest off-axis angle with respect to the INTEGRAL pointing direction, near to the edge of the FoV of both main instruments, IBIS and SPI. Nevertheless, it was possible to determine its position and to extract spectra and fluxes. The GRB nature of the event was confirmed by an IPN triangulation. It is a ∼60 s long GRB with two prominent peaks separated by ∼35 s. The spectral shape of the GRB is best represented by a single power law with a photon index $\Gamma \simeq 1.7$. The peak flux in the 20–200 keV band is determined to ∼5.7 photons cm^{-2} s^{-1} and the GRB fluence to 1.1×10^{-5} erg cm^{-2}. Analysing the spectral evolution of the GRB, a "hard-to-soft" behaviour emerges. A search for an optical counterpart has been carried out, but none was found.

Key words. gamma-ray bursts – GRB – gamma-ray astronomy – INTEGRAL – SPI – IBIS

1. Introduction

Since their discovery more than thirty years ago (Klebesadel 1973) GRBs had evaded an understanding of their nature for about 20 years. This changed dramatically with the identification of the first GRB X-ray afterglow with a BeppoSAX observation (Costa et al. 1997). Since then it has been shown that at least the sources of long GRBs (lasting longer than 2 s) are located at cosmological distances. The observed fluxes revealed the enormous energy release of these events (van Paradijs et al. 2000) which is thought to be produced in asymmetric collapse of massive stars (Woosley 1993).

Here we report the detection of such an event by the two main instruments of INTEGRAL (Winkler et al. 2003) which have complementary performance characteristics. The imager IBIS (Ubertini et al. 2003) has an excellent angular resolution, whereas the spectrometer SPI (Vedrenne et al. 2003) is assigned to high-resolution spectroscopy, but has only modest imaging capabilities. The burst-detection capabilities of the INTEGRAL mission are achieved by the INTEGRAL burst alert system (IBAS: Mereghetti et al. 2003a; IBAS for SPI/ACS: von Kienlin et al. 2001), which scans the satellite telemetry in near-real time for GRBs at the INTEGRAL Science Data Centre (ISDC; Courvoisier et al. 2003).

2. Detection and localisation

On March 20, 2003 at 10:11:40 UTC, during the Galactic Centre Deep Exposure, a long GRB (∼60 s) was detected at a large off-axis angle of 15.5°. This is near to one corner of the squared shaped IBIS FoV: 29° × 29° full width (SPI-FoV: ∼35° full width).

Send offprint requests to: A. von Kienlin,
e-mail: azk@mpe.mpg.de

⋆ Based on observations with INTEGRAL, an ESA project with instruments and science data centre funded by ESA member states (especially the PI countries: Denmark, France, Germany, Italy, Switzerland, Spain), Czech Republic and Poland, and with the participation of Russia and the USA and on observations made with ESO telescopes at the La Silla Observatory under programme Id 71.D-0667(C).

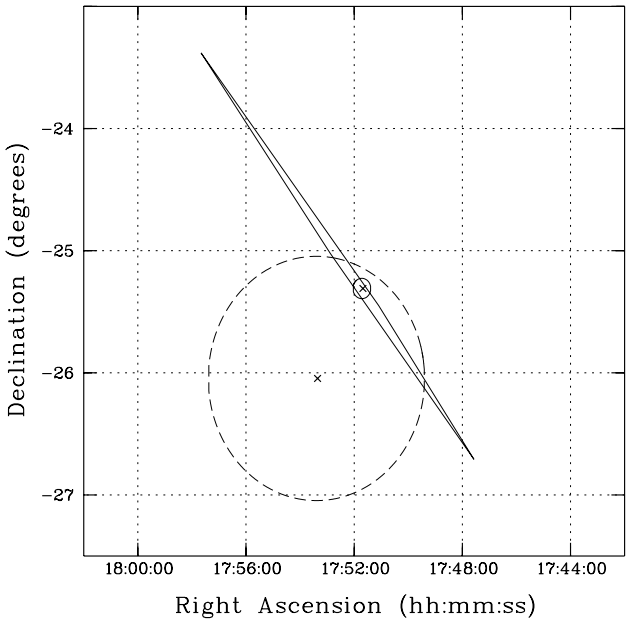

Fig. 1. Localisations of GRB 030320 showing the IBIS/ISGRI position (central cross) and error circle (solid line) of Mereghetti et al. (2003b). The IPN error box of Hurley et al. (2003b) and the derived SPI position with its 1° error circle (dashed line) are superimposed.

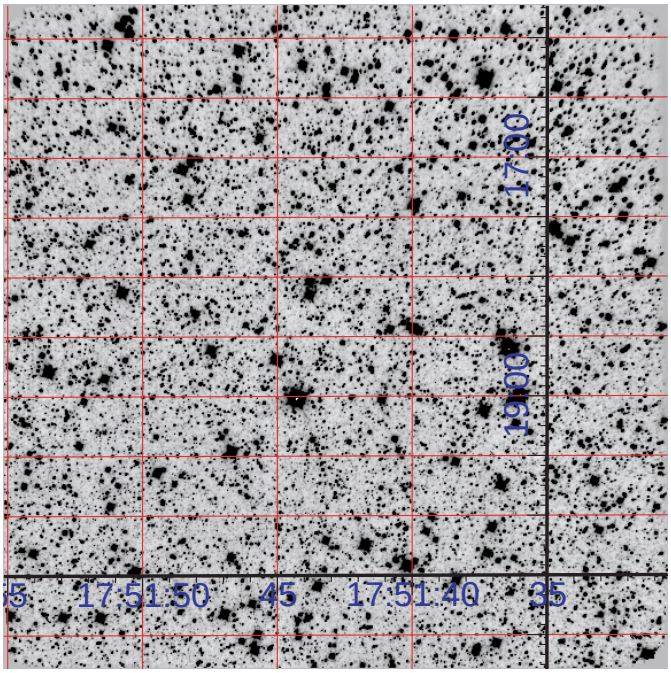

Fig. 2. ESO/NTT+SOFI image corresponding to the centre of the IBIS error circle derived here. The field is 5.5 × 5.5 arcmin wide. The 5 σ limiting magnitude is Ks = 20.7.

The GRB was detected by IBAS in near-real time in the data of ISGRI (Lebrun et al. 2001), the low-energy detector of IBIS. As the trigger had a low significance due to the position of the source on the edge of the FoV (only 3.7% of the detector was illuminated by the GRB) no prompt alert was distributed. An offline interactive analysis of the data confirmed that the trigger was due to an astrophysical source and allowed to determine and distribute a preliminary position 6.25 hours after the event (IBAS Alert 343; Mereghetti et al. 2003b). The preliminary derived position was $\alpha_{J2000} = 17^h51^m43^s$, $\delta_{J2000} = -25°18'34''$ with an uncertainty of 5′. In a further analysis of the entire GRB (UTC 10:11:36–10:12:40) in the 15–100 keV energy band the GRB was detected with a signal-to-noise ratio of $S/N \sim 15$. The derived error box had nearly the same centre $\alpha_{J2000} = 17^h51^m42^s$, $\delta_{J2000} = -25°18'44''$ but a smaller radius of 3′.

The GRB nature of the event was confirmed about one hour later by Konus, Mars Odyssey (HEND), and INTEGRAL/SPI-ACS via an IPN-annulus (Hurley et al. 2003a). By adding the information from Ulysses, Mars Odyssey (GRS), Konus-Wind and RHESSI to the above mentioned data, a small IPN error box was derived one day later (Hurley et al. 2003b).

SPI was only able to determine a rough position for the GRB in the energy interval between 100 keV and 1 MeV. At lower energies it was not possible to derive a position. One should notice that only 3 out of the 19 detectors of SPI's camera showed a substantial increase of the count rate, caused by the illumination of the GRB. By selecting two time intervals around the prominent peaks of emission (see below) from UTC 10:11:55 to 10:12:05 and 10:12:30 to 10:12:36 (in total 16 s), the derived SPI position is $\alpha_{J2000} = 17^h53.4^m$, $\delta_{J2000} = -26°2.8'$ with an uncertainty of 1° (S/N 7.2). This agrees within the error with the positions found by IBIS/ISGRI and IPN. Figure 1 shows a superposition of the IPN error box and the SPI- and IBIS/ISGRI-error circles.

The two monitoring instruments of INTEGRAL, the X-ray monitor JEM-X (Lund et al. 2003) and the optical camera OMC (Mas-Hesse et al. 2003), did not observe the event as it was outside their FoVs.

A search for an optical afterglow in the IBIS error circle was performed using the Wise-Observatory 1 m telescope 16.9 hours after the onset of the burst (Gal-Yam & Ofek 2003). This follow-up observation did not reveal any optical counterpart. R-band imaging under poor conditions did not show any new source down to a limiting magnitude of $R = 17.5$ mag.

We also performed two follow-up observations at ESO New Technology Telescope (NTT) using the SOFI camera. The first was made at 9.497 UT on the 21st of March (~23.3 hours after the GRB) with a Ks filter and had exposure of 30 min (see Fig. 2). The second was taken at 4.608 UT (~69.8 days after the GRB) on the 29th of May with the same filter and an exposure of 10 min. The difference image, although showing several variable sources, did not reveal a strong afterglow candidate.

The afterglow search was complicated by the burst location in the galactic plane. The foreground galactic hydrogen column density[1] of $N_H = (1.4 \pm 0.1) \times 10^{22}$ atoms/cm^2 in the direction of the burst results in an extinction of $A_V = (10.5 \pm 0.5)$ mag [$A_R = (7.85 \pm 0.35)$ mag]. This high extinction would have required an extraordinary intrinsically bright afterglow ($R_{int} < 10$ mag at the time of the Wise observations) in order to be detectable. This would be more than 5 mag brighter than the

[1] http://heasarc.gsfc.nasa.gov/cgi-bin/Tools/w3nh/w3nh.pl

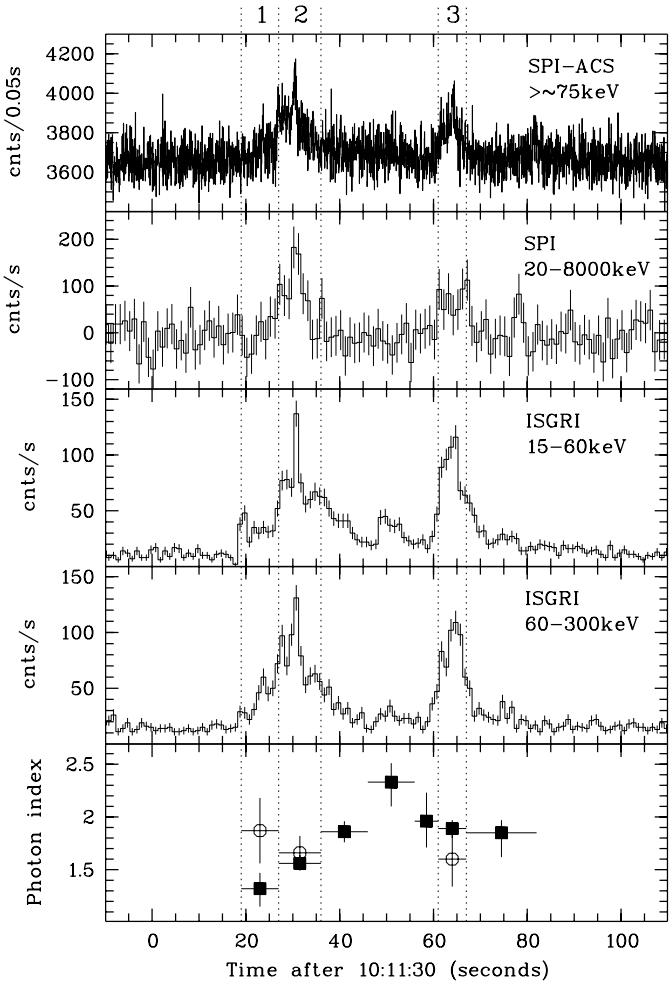

Fig. 3. Lightcurves of all INTEGRAL instruments which have seen GRB030320, from top to bottom: SPI-ACS overall veto count rate with 50 ms time resolution, SPI 1 s binned and IBIS/ISGRI in a soft (15–60 keV) and a hard (60–300 keV) energy range with 1 s binning. The bottom plot shows the evolution of photon index Γ [$f(E) = K \cdot (\frac{E}{1\mathrm{keV}}^{-\Gamma})$; K = photons/(keV cm^2 s) at 1 keV] for ISGRI (filled square) and SPI (XSPEC 12.0 results, open circle). The dotted lines mark the intervals 1–3 from Table 1.

very bright afterglow of GRB 030329 (Burenin et al. 2003) at the same time after the burst occurrence.

3. Temporal and spectral characteristics

Figure 3 shows the lightcurve for all INTEGRAL detectors which have observed GRB 030320. The lightcurves of ISGRI have been determined in two energy bands (15–60 keV and 60–300 keV) by using only the pixels that were illuminated by the GRB by at least half of their surface. The determination of a SPI lightcurve with a short time binning was only possible by using the 1 s count rates of the 19 Ge-detectors, which are normally used for science-housekeeping purposes. These values reflect the count rates of each detector in the broad SPI energy band from ∼20 keV up to ∼8 MeV. The SPI lightcurve in Fig. 3 was generated by summing the background-subtracted count rates. The background (∼50 counts s^{-1} detector^{-1}) was determined from the SPI data before the burst occurrence over a duration of 40 min. The alternative method, which uses the time-tagged photon-by-photon SPI mode, with energy information for each photon, yielded insignificant results. With the anti-coincidence shield (ACS) of SPI the GRB was observed as an increase of the overall veto count rate. The effective area of the ACS is very small for sources observed within the field of view (von Kienlin et al. 2003a). For GRBs which occur outside the FoV of SPI the effective area of the ACS is however large, as it can be seen from the detection rate of ∼0.8 GRBs/day (von Kienlin et al. 2003b). All lightcurves in Fig. 3 exhibit two prominent peaks during the ∼60 s of prompt emission. A third peak is visible in the low-energy range of ISGRI, which is less significant at higher energies.

Spectra were extracted for characteristic intervals of the GRB lightcurve. The GRB spectrum was in all cases well represented by a single power-law model. The photon index and the source flux in the 20–200 keV energy range are listed for ISGRI and SPI in Table 1. For both instruments, the response for a source position near-to-zero coding is not yet well understood. For ISGRI the closest Crab observation was used for the calibration of the spectra. Any deficiencies of the SPI response at 15.5° off-axis angle is possibly the result of a not fully-representative mass model. Currently the off-axis effects of the response are assessed by using Crab observations, recorded during the payload-verification campaign, but the drawback of this method is the lack of Crab observations at such large off-axis angles.

The photon indices and fluxes listed in Table 1 for SPI were obtained by binning the photon-by-photon single and multiple events into six equally-spaced logarithmic energy bins in the 20 keV to 2 MeV range, for each of the listed time intervals. Spectral extraction was performed using SPIROS (SPI Iterative Removal of Sources; Skinner & Connell 2003), which takes the SPI photopeak effective area into account. Spectral model fitting was performed using XSPEC 11.2 and the off-diagonal response of SPI (SPI-RMF), as shown in the line $\mathrm{SPI}^{\mathrm{offd.}}_{11.2}$ of Table 1. For the background, all event data of the corresponding science window, with a duration of about 30 min, were used, but with the time of the GRB cut out (UTC 10:11:40–10:14:00). Table 1 lists the obtained photon indices and fluxes, when using XSPEC 11.2 only with a diagonal response (line $\mathrm{SPI}^{\mathrm{diag.}}_{11.2}$) too. Naturally one obtains a softer spectral shape with this method.

For comparison, the data were analysed using an alpha-test version of the XSPEC 12.0 software. This approach is distinct from the SPIROS method, in that the full diagonal plus off-diagonal response matrix is computed for each detector (and for each pointing direction, although here the GRB is contained within a single pointing) (Sturner et al. 2003; also Shrader et al. 2000). The detector-count spectra are then compared directly to the convolution of a photon model with, in this case, 19 response matrices, and a χ^2 minimisation is performed. This is, in principle, a more rigorous deconvolution procedure than the SPIROS method. However, the disadvantage is that the source and background must be simultaneously modelled whereas SPIROS reduces the problem to a single background subtracted spectrum and response matrix. A set of ancillary

Table 1. Photon indices and fluxes obtained by IBIS/ISGRI and SPI (by three different methods, see text) in 6 time intervals of the GRB. The quoted uncertainties are given for a 90% confidence range. For line $SPI_{12.0}$ it was only possible to quote the 90% confidence range approximately, because the calculation of uncertainty contours is not yet implemented in XSPEC 12.0.

Interval #		1	2	3	4	5	6
Position		before 1st peak	1st peak	2nd peak	max 1st peak	#1 + #2	full GRB
UTC 10 : __ : __		11:49–11:57	11:57–12:06	12:31–12:37	12:00–12:02	11:49–12:06	11:49–12:37
PhoIndex	ISGRI	$1.32\,^{0.15}_{-0.17}$	$1.56\,^{0.08}_{-0.07}$	$1.89\,^{0.09}_{-0.09}$	$1.62\,^{0.08}_{-0.09}$	$1.52\,^{0.08}_{-0.08}$	$1.69\,^{0.07}_{-0.08}$
	$SPI_{12.0}$	1.87 ± 0.31	1.66 ± 0.16	1.60 ± 0.26	1.01 ± 0.31	1.54 ± 0.15	1.51 ± 0.16
	$SPI^{offd.}_{11.2}$	$1.68\,^{0.67}_{-0.67}$	$0.94\,^{0.45}_{-0.87}$	$1.29\,^{0.45}_{-0.64}$	–	$1.28\,^{0.35}_{-0.48}$	$1.19\,^{0.29}_{-0.37}$
	$SPI^{diag.}_{11.2}$	$1.97\,^{0.71}_{-0.47}$	$1.40\,^{0.25}_{-0.28}$	$1.56\,^{0.36}_{-0.38}$	$1.03\,^{0.43}_{-0.50}$	$1.54\,^{0.24}_{-0.25}$	$1.57\,^{0.20}_{-0.20}$
20–200 keV Flux $\left[\frac{ph}{cm^2 s}\right]$	ISGRI	1.449	3.841	3.685	5.689	2.773	2.068
	$SPI_{12.0}$	3.08	4.35	3.53	3.14	3.24	2.11
	$SPI^{offd.}_{11.2}$	3.62	2.05	3.56	–	2.78	1.65
	$SPI^{diag.}_{11.2}$	4.40	4.45	4.95	4.13	4.11	2.82

response functions (ARFs), containing the energy, detector and angle-dependent effective area, were constructed for the GRB position and the burst spectrum was modelled in XSPEC 12.0 by fixing the background (derived by using the non-burst part of the observation). The obtained photon indices and fluxes are listed in the line $SPI_{12.0}$ of Table 1.

ISGRI single events have been used to derive photon indices and fluxes shown in the line "ISGRI" of Table 1. Thanks to the coded-mask design of the IBIS telescope, the source flux can be determined simultaneously with the background using the Pixel Illumination Function (PIF; Skinner 1995). The spectra have been extracted in 128 linearly-spaced energy bins between 19 keV and 1 MeV and were rebinned to have a signal-to-noise ratio larger than 3 in each channel. The photon spectra have then been obtained with the technique described above. In addition to the time intervals shown in Table 1 it was possible to obtain for ISGRI values of the photon index for the time intervals listed below:

Position:	Interval (UTC)	PhoIndex
decay of the 1st peak:	10:12:06–10:12:16	$1.859\,^{0.10}_{-0.10}$
small peak in between:	10:12:16–10:12:26	$2.329\,^{0.18}_{-0.23}$
rising of the 2nd peak:	10:12:26–10:12:31	$1.955\,^{0.28}_{-0.25}$
decay of the 2nd peak:	10:12:37–10:12:52	$1.849\,^{0.22}_{-0.22}$

With these ISGRI data it was possible to track the spectral evolution over the whole emission period, showing a general hard-to-soft evolution for the first peak up to the small peak between the two main peaks (Fig. 3 lower panel). During the second peak the spectrum hardens again (yet being softer compared to the first peak), but showing no evolution. The obtained ISGRI fluxes are reasonably correlated with the light curve.

The photon indices obtained with XSPEC 12.0 for SPI agree within the errors with the results obtained with ISGRI for interval 2, 3, 5 and 6, but reveals no spectral evolution. In contrast to the time between interval 2 and 3 (between to two main peaks) and after the last interval 3 (decay of the 2nd peak), it was possible to extract for SPI a spectrum for interval 1, although SPI's lightcurve did not show a rate increase. As expected the obtained photon index and flux do not agree well with the ISGRI values. A large discrepancy is observed for interval 4 (maximum of the 1st peak). SPI shows here a rather hard spectrum whereas for ISGRI the spectrum is even softer compared to interval 5. The SPI results have to be handled with care because for such a short 2 s interval, containing only a small number of counts in each energy bin, the determination of a spectrum is more difficult.

Comparing the results obtained with the three different methods used for the SPI data analysis, one can see that the XSPEC 12.0 derived photon indices yield the best agreement with the ISGRI data, although the same is valid for the SPIROS+XSPEC 11.2 results, using a diagonal response (line $SPI^{diag.}_{11.2}$ of Table 1), but these have a much broader confidence range. Second it should be noted that XSPEC 12.0 is using an off-diagonal response, which should represent the instrument much better.

The burst had a 20–200 keV peak flux (over 2 s) of $4.1\,^{1.3}_{-1.4} \times 10^{-7}$ erg cm^{-2} s^{-1} and 5.4×10^{-7} erg cm^{-2} s^{-1} and a 25–100 keV peak flux of $1.7\,^{0.9}_{-0.7} \times 10^{-7}$ erg cm^{-2} s^{-1} and 3.0×10^{-7} erg cm^{-2} s^{-1} measured with SPI and IBIS/ISGRI, respectively. These peak fluxes would place GRB 030320 in the top 25% of the BATSE peak flux distribution (Paciesas et al. 1999).

The gamma-ray fluence in the 20–200 keV band measured with SPI is $1.35\,^{0.21}_{-0.26} \times 10^{-5}$ erg cm^{-2}, consistent with 1.1×10^{-5} erg cm^{-2} from IBIS/ISGRI. The 25–100 keV fluence was $7.1\,^{1.6}_{-1.8} \times 10^{-6}$ erg cm^{-2} (SPI) and 6.5×10^{-6} erg cm^{-2} (ISGRI). Peak flux and fluence agree within a factor of two with the results obtained with Ulysses (Hurley et al. 2003b).

4. Conclusion

The analysis of GRB 030320 showed that INTEGRAL is still able to detect GRBs at the edge of its FoV. For this GRB a photon index of $\Gamma \simeq 1.7$ was derived for the prompt emission. The time resolved spectroscopy revealed a hard-to-soft transition of the spectrum during the 60 burst duration. Especially

IBIS/ISGRI showed a good performance in localisation and in the determination of the spectral evolution. The difficulties observed with SPI will hopefully improve with a better understanding of the response at the edge of the FoV.

Acknowledgements. The SPI project has been completed under the responsibility and leadership of CNES. We are grateful to ASI, CEA, CNES, DLR, ESA, INTA, NASA and OSTC for support. The SPI/ACS project is supported by the German "Ministerium für Bildung und Forschung" through DLR grant 50.OG.9503.0.

References

Burenin, R. A., Sunyaev, R. A., Pavlinsky, M. N., et al. 2003, Astron. Lett., accepted [astro-ph/0306137]
Coburn, W., & Boggs, S. E. 2003, Nature, 423, 415
Costa, E., Frontera, F., Heise, J., et al. 1997, Nature, 387, 783
Courvoisier, T. J.-L., Walter, R., Beckmann, V., et al. 2003, A&A, 411, L53
Gal-Yam, A., & Ofek, E. O. 2003, GCN, 1946
Hurley, K., Cline, T., Mitrofanov, I., et al. 2003a, GCN, 1942
Hurley, K., Cline, T., Mitrofanov, I., et al. 2003b, GCN 1943
Klebesadel, R., Strong, I., & Olsen, R. 1973, ApJ, 182, L85
Lebrun, F. 2001, in Proc. 4th INTEGRAL Workshop, ESA SP 459, 591
Lund, N., Brandt, S., Budtz-Jorgensen, C., et al. 2003, A&A, 411, L231
Mas-Hesse, M., Gimenez, A., Culhane, L., et al. 2003, A&A, 411, L261
Mereghetti, S., Götz, D., Borkowski, J., et al. 2003a, A&A, 411, L291
Mereghetti, S., Götz, D., Borkowski, J., et al. 2003b, GCN, 1941
Paciesas, W. S., Meegan, C. A., Pendleton, G. N., et al. 1999, ApJS, 122, 465
van Paradijs, J., Kouveliotou, C., & Wijers, R. A. M. J. 2000, ARA&A, 38, 379
Shrader, C., Sturner, S., & Teegarden, B. 2000, Proc. The Fifth Compton Symp., AIP CP-510
Skinner, G. K. 1995, Experimental Astronomy, 6/4, 1
Skinner, G. K., & Connell, P. H. 2003, A&A, 411, L123
Sturner, S., Shrader, C. R., Weidenspointner, W., et al. 2003, A&A, 411, L81
Ubertini, P., Lebrun, F., Di Cocco, G., et al. 2003, A&A, 411, L131
Vedrenne, G., Roques, J.-P., Schönfelder, V., et al. 2003, A&A, 411, L63
von Kienlin, A., Arend, N., & Lichti, G. G. 2001, in Proc. of the International GRB workshop held in Rome (Springer), 427
von Kienlin, A., Arend, N., Lichti, G. G., et al. 2003, in SPIE Conf. Proc. 4851, X-ray and Gamma-ray Telescopes and Instruments for Astronomy, 1336
von Kienlin, A., Beckmann, V., Rau, A., et al. 2003, A&A, 411, L299
Winkler, C., Courvoisier, T. J.-L., Di Cocco, G., et al. 2003, A&A, 411, L1
Woosley, S. E. 1993, ApJ, 405, 273